

## Multiexcitons confined within a subexcitonic volume: Spectroscopic and dynamical signatures of neutral and charged biexcitons in ultrasmall semiconductor nanocrystals

M. Achermann, J. A. Hollingsworth, and V. I. Klimov

*Chemistry Division, C-PCS, MS-J585, Los Alamos National Laboratory, Los Alamos, New Mexico 87545, USA*

(Received 20 June 2003; published 3 December 2003)

The use of ultrafast gating techniques allows us to resolve both spectrally and temporally the emission from short-lived neutral and negatively charged biexcitons in ultrasmall (sub-10 nm) CdSe nanocrystals (nanocrystal quantum dots). Because of “forced” overlap of electronic wave functions and reduced dielectric screening, these states are characterized by giant interaction energies of tens (neutral biexcitons) to hundreds (charged biexcitons) of meV. Both types of biexcitons show extremely short lifetimes (from sub-100 picoseconds to sub-picosecond time scales) that rapidly shorten with decreasing nanocrystal size. These ultrafast relaxation dynamics are explained in terms of highly efficient nonradiative Auger recombination.

DOI: 10.1103/PhysRevB.68.245302

PACS number(s): 78.67.Bf, 42.50.Hz, 73.22.-f, 78.47.+p

In ultrasmall, sub-10 nm semiconductor nanocrystals [known also as nanocrystal quantum dots (QDs)], new types of strongly interacting multiexciton states can exist that do not occur in “natural” bulk semiconductors. The interaction strength in the multiexciton system scales directly with the excitation density (i.e., the number of excitons per  $\text{cm}^3$ ). However, in bulk materials, there is a fundamental limit on maximum densities for which excitons still exist. This limit corresponds to the exciton dissociation threshold ( $n_{th}$ ) which is roughly determined by densities corresponding to one exciton per excitonic volume:  $n_{th} \sim a_B^{-3}$ , where  $a_B$  is the exciton Bohr radius. Above this threshold, a dielectric excitonic gas transforms into metallic electron-hole ( $e-h$ ) plasmas, and the Coulomb interactions become greatly reduced because of strong dynamic screening by unbound charge carriers.<sup>1</sup>

In contrast to the bulk case, in semiconductor nanoparticles one can generate states in which several excitons occupy a volume comparable to or smaller than the volume of a bulk exciton. Such “squeezed” exciton states are characterized by greatly enhanced multiparticle interactions resulting from a *forced* overlap of electronic wave functions and reduced dielectric screening. The latter effect occurs because of a penetration of the electric field outside a nanoparticle (the surrounding medium is typically characterized by a lower dielectric constant) and reduced efficiency of dynamic screening (carriers are locked in the nanoparticle by rigid boundary conditions which result in low electronic polarizability).

In addition to revealing new physics, studies of strongly interacting multiexcitons are relevant to several emerging technologies. For example, optical amplification and lasing in sub-10 nm nanocrystals rely on emission from particles occupied with two or more excitons.<sup>2,3</sup> Therefore, the control of optical gain properties of nanocrystal QDs requires detailed understanding of energy spectra and dynamics of strongly confined multiexcitons. Another example involves quantum technologies in which two excitons in a quantum dot can be used as a quantum-bit pair<sup>4</sup> for quantum information processing or as a source of entangled photon pairs.<sup>5</sup>

The challenge in experimentally detecting spectroscopic signatures of strongly confined multiexcitons is associated

with their very short (picoseconds to hundreds of picoseconds) lifetimes that are limited by nonradiative, multiparticle Auger recombination.<sup>6</sup> Because these times are significantly shorter than the radiative decay time, multiexcitons are undetectable in time-integrated (cw) photoluminescence (PL) spectra. In this paper, we report for the first time the emission spectra of strongly confined neutral and charged biexcitons in sub-10 nm CdSe QDs detected using time-resolved, femtosecond PL measurements. These multiexciton states are manifested in femtosecond PL spectra as two bands observed in addition to a single-exciton emission line. Both bands are characterized by a superlinear pump-intensity dependence indicating their multiexcitonic origin. The detected states are also characterized by extremely large interaction energies (tens to hundreds of meV) which can be explained by the existence of strong *attractive* forces between squeezed excitons. Since the observed interaction energies are comparable to or even greater than room-temperature thermal energies, ultrasmall, sub-10 nm quantum dots can be used for room-temperature implementations of quantum technologies that are based on multiexciton interactions.

QDs used for this study are highly monodisperse, chemically synthesized CdSe nanocrystals overcoated with a ZnS shell and a final layer of organic ligand molecules (core-shell nanocrystal QDs). We investigated seven samples with a narrow size dispersion of 5–7 % and mean dot radii from 1.1 to 3.6 nm which corresponds to  $0.2-0.8a_B$ . The samples are excited at 400 nm by the frequency-doubled output of an amplified Ti:sapphire laser (250 kHz repetition rate). Ultrafast, time-resolve PL measurements are performed using a femtosecond PL up-conversion (uPL) technique.<sup>7</sup> In these measurements, the emission from QDs is frequency-mixed (gated) with 200 fs pulses of the fundamental laser radiation in a nonlinear-optical  $\beta$ -barium borate crystal. The sum frequency signal is spectrally filtered with a monochromator and detected using a cooled photomultiplier tube coupled to a photon counting system. The time resolution of uPL measurements is  $\sim 300$  fs. All measurements are performed at room temperature.

The need for a short time-resolution for detecting multiexciton states in strongly confined QDs becomes evident from data in Fig. 1(a), in which we compare a cw PL spec-

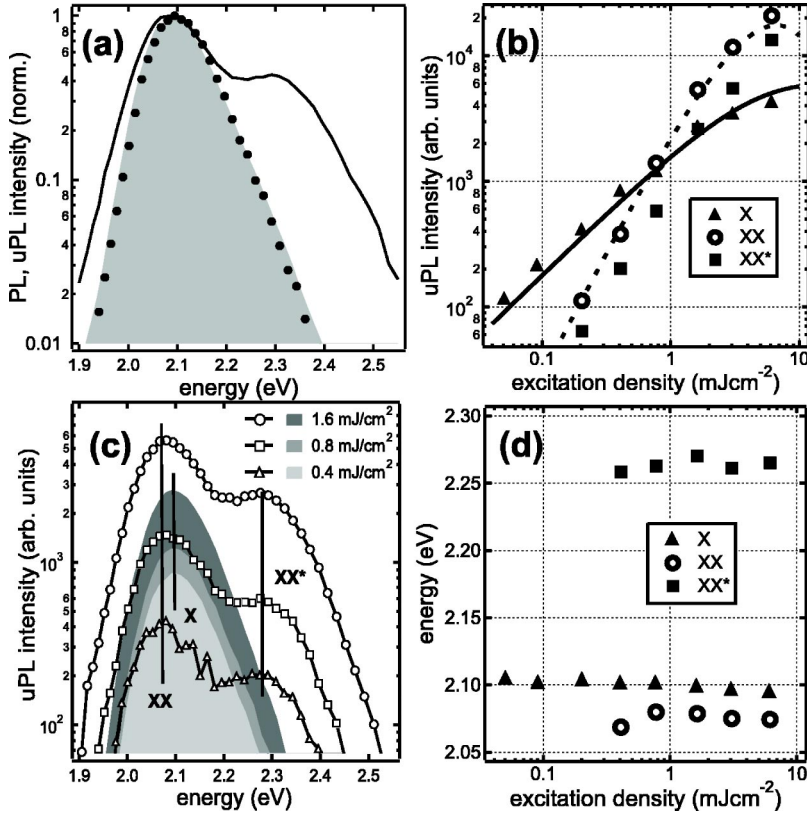


FIG. 1. (a) Normalized time-integrated (shaded area) and time-resolved uPL spectra ( $w_p = 3.4$  mJ cm $^{-2}$ ) measured at  $\Delta t = 1$  ps (solid line) and  $\Delta t = 200$  ps (solid circles). (b) Pump-intensity dependence of X (triangle), XX (circles), and XX\* (squares) band amplitudes compared to fitting curves (lines) calculated assuming the Poisson distribution of QD populations (see text for details). (c) Single exciton (shaded areas) and multiexciton (symbols) emission spectra (extracted from the 1 ps uPL spectra) at different excitation densities. (d) Pump-intensity dependence of the spectral positions of the X (triangle), XX (circles), and XX\* (squares) bands.

trum with the uPL spectra measured at  $\Delta t = 1$  ps and 200 ps after excitation. All these spectra were recorded at the same pump fluence ( $w_p$ ) of 3.4 mJ cm $^{-2}$ , which corresponds to the excitation of more than 10 excitons per dot on average. Because of fast nonradiative Auger recombination, all multiexcitons decay on a sub-100 ps time scale<sup>6</sup> and, therefore, the uPL spectrum at  $\Delta t = 200$  ps [circles in Fig. 1(a)] is entirely due to single-exciton emission. Interestingly, this spectrum is essentially identical to the cw spectrum [shaded area in Fig. 1(a)], indicating that time-integrated emission is dominated by single excitons even in the case of high excitation levels for which several excitons are initially generated in a significant number of dots. The early-time uPL spectrum recorded at  $\Delta t = 1$  ps [solid line in Fig. 1(a)] is distinctly different from the excitonic emission and displays a clear shoulder on the low-energy part of the excitonic band and a new high-energy emission band. These new features only develop at high excitation densities that correspond to an average number of  $e-h$  pairs (excitons) per dot  $\bar{N} > 1$  and, therefore, should be attributed to multiexciton states as analyzed below [ $\bar{N}$  is estimated from the expression  $\bar{N} = \sigma_a(w_p/\hbar\omega_p)$ , where  $\sigma_a$  is the QD absorption cross section at the pump spectral energy  $\hbar\omega_p$ ; Ref. 8].

In the analysis of high-pump-intensity PL spectra, we assume the Poisson distribution of initial QD populations. This distribution accurately describes photoexcited QD ensembles in the case of femtosecond pumping well above the energy gap when the probability for generating a new  $e-h$  pair in a dot is independent of the number of pairs already existing in this dot.<sup>8</sup> For the Poisson distribution, the concentration of QDs that contain  $N$  excitons ( $n_N$ ) immediately following excitation

with an ultrashort laser pulse is expressed as  $n_N = n\bar{N}^N e^{-\bar{N}}/N!$ , where  $n$  is the total concentration of QDs in the sample. While the intrinsic decay of singly excited CdSe nanocrystals occurs due to radiative recombination, which is characterized by the time constant  $\tau_r \approx 20$  ns at room temperature,<sup>9</sup> the multiexciton decay is primarily due to much faster nonradiative Auger recombination with time constants  $\tau_A \lesssim 200$  ps for the QD sizes studied.<sup>6</sup> Since the decay of QD multiexcitons eventually produces a singly excited dot, the concentration of excitons ( $n_X$ ) at intermediate time delays  $\tau_A < \Delta t < \tau_r$  is determined by the total number of dots excited by a pump pulse (independent of the initial number of excitations per dot) and, hence, can be estimated from the expression  $n_X = n - n_0 = n(1 - e^{-\bar{N}})$ . This expression closely reproduces the pump dependence of the PL intensity measured at the center of the exciton band at  $\Delta t = 200$  ps [compare solid triangles (experiment) and solid line (model) in Fig. 1(b)] indicating the validity of the above considerations.

In order to extract the multiparticle component from uPL spectra, one needs to account for a contribution from singly excited QDs at early times after excitation. We calculate this contribution by scaling the purely excitonic spectra detected at time delays  $\Delta t > \tau_A$  ( $\Delta t = 200$  ps in our experiments) by two factors. One factor accounts for a single-exciton decay (derived from the PL dynamics measured at low excitation intensities corresponding to  $\bar{N} < 1$ ) and the other describes a contribution from additional single exciton states produced as a result of the multiexciton decay. In the case of the Poisson distribution, the latter factor can be calculated as  $n_1/n_X = \bar{N}/(e^{\bar{N}} - 1)$ .

In Fig. 1(c), we show, by shaded areas, pump dependent uPL spectra recorded at  $\Delta t = 200$  ps; as discussed earlier, these spectra correspond to the purely single-exciton emission. By scaling the 200 ps spectra according to the procedure described above and subtracting them from early time spectra measured at 1 ps, we extract the spectral component that is entirely due to the multiexciton emission [symbols in Fig. 1(c)]. The multiexciton spectra show two bands: one (XX) on the low and the other (XX\*) on the high energy side of the exciton (X) line (the multiexciton band notations are clarified below). The positions of XX and XX\* bands<sup>10</sup> are independent of the pump power [Fig. 1(d)], indicating that each of these bands is due to emission from dots in a well-defined multiparticle state rather than due to superposition of emission spectra from dots with different numbers of photoexcitations (in the latter case, the positions/shapes of the spectra should show pump dependence).

In Fig. 1(b), we compare the pump dependence of the XX and XX\* bands (open circles and solid squares, respectively) with that measured for a single-exciton band (solid triangles). While the single-exciton emission shows a linear initial growth (with respect to  $w_p$ ), the initial growth is *quadratic* for both multiexciton bands, indicating an excitation mechanism that involves absorption of two photons from the same pump pulse. This quadratic mechanism is also confirmed by the fact that the pump dependence over the entire range of intensities (including the saturation region at high pump levels) can be closely modeled in terms of the Poisson distribution assuming that the multiexciton emission is due to doubly excited QDs [i.e., is described by the term  $n_2 = (nN^2/2)e^{-N}$ ].

Despite identical pump dependencies, the XX and XX\* bands likely originate from different types of biexciton states because of their very different spectral positions. The low energy XX band is located immediately below the single-exciton line, which allows us to assign it to the emission of a biexciton, in which both electrons are in the lowest 1S state (the  $1S_e^2$  biexciton). Such biexcitons are generated via absorption of two photons by a dot that was not occupied prior to the arrival of a pump pulse. The biexcitonic assignment of the XX feature is also confirmed by the analysis of its dynamics. As shown below, size dependent decay times of the XX band closely match those measured for two electron-hole pair states in Ref. 6 using a transient absorption experiment.

The spectral position of the second, high-energy multiexciton band indicates that it likely involves the emission from the excited (1P) electron state. Because of fast, subpicosecond 1P-to-1S relaxation,<sup>11</sup> the occupation of the 1P state can only be stabilized if the 1S orbital is fully filled (i.e., contains two electrons). This suggests that the high-energy band is not due to excited neutral biexcitons but rather due to charged biexciton states (XX\*) involving two holes and three electrons, with the electron-shell configuration  $1S_e^2 1P_e^1$ . The observed XX\* emission originates likely from the  $1P_e - 1S_{h,3/2}$  transition, which is nominally forbidden, but can be allowed in multiexciton states due to Coulomb interactions.<sup>12</sup> It is also possible that the thermally populated  $1P_{h,3/2}$  hole state is involved in this emission (transition  $1P_e - 1P_{h,3/2}$ ).

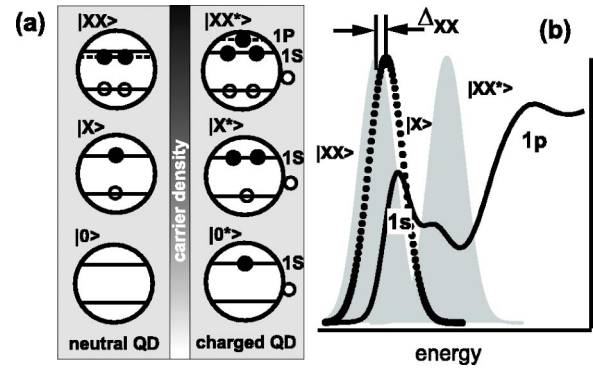


FIG. 2. (a) A cartoon illustrating the progression of states that develops in neutral and charged dots with increasing pump level. (b) A schematic illustration of neutral (XX) and charged (XX\*) biexciton emission spectra compared to a single exciton PL spectrum (X) (solid circles) and a typical absorption spectrum of CdSe nanocrystal QDs (1S and 1P are two strong optical transitions that involve the lowest and the first excited electron states and  $\Delta_{XX}$  is the biexciton binding energy).

The fact that the XX\* states are excited via a “quadratic” process can be explained by the existence of a subensemble of dots with long-lived 1S electrons that “survive” on time scales comparable to or longer than the time separation between two sequential pump pulses (4  $\mu$ s in our case). Since excitons decay radiatively on a nanosecond time scale, long-lived 1S electrons are likely associated with charge-separated electron-hole pairs formed, e.g., as a result of hole surface trapping.<sup>8</sup> The efficiency of surface trapping correlates with PL quantum yields (QYs), suggesting that the intensity of the XX\* band should increase as the QY is decreased. This is exactly the trend we observe in our experiments using samples with differently prepared surfaces (e.g., purely organic passivation vs ZnS overcoating). Furthermore, the existence of dots that contain long-lived charges (charged dots) has been previously suggested based on results of single-QD PL intermittence<sup>13</sup> and QD charging experiments.<sup>14</sup>

Our model that explains two multiexciton features in terms of two subensembles of *neutral* and *charged* dots is schematically depicted in Fig. 2. In this model, both the excitonic (X) and the biexcitonic (XX) features originate from neutral dots (no charges prior to the arrival of a pump pulse) while the charged biexciton (XX\*) feature is generated by adding two excitons into a charged dot that already contains an electron in the 1S state and a hole in a surface state.

Since we clearly observe XX\* species, one would expect that charged excitonic X\* species should also be observed in our experiments. The fact that this type of state is not clearly manifested in uPL spectra is likely because their emission spectrally overlaps with the emission from either X or XX states. On the other hand, we do observe some indirect dynamical signatures of X\* species such as a fast initial decay of the PL signal observed when nominally less than one exciton per dot is excited. In addition to ultrafast processes such as carrier surface trapping, this fast initial decay may be due to ultrafast Auger recombination of charged excitons.

In bulk CdSe, excitons are weakly attractive and form

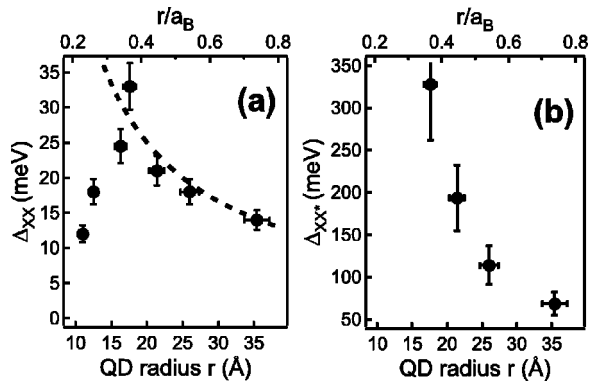


FIG. 3. QD size dependence of the neutral  $\Delta_{XX}$  (a) and charged  $\Delta_{XX^*}$  (b) biexciton energy shifts ( $a_B \approx 48$  Å in bulk CdSe). The  $\Delta_{XX}$  size dependence [panel (a)] in the range  $r \geq 17$  Å is fit to  $1/r$  (dashed line).

biexcitons with a binding energy  $\delta E_2 \approx 4.5$  meV.<sup>15</sup> Strong 3D quantum confinement and reduced dielectric screening have been expected to strongly modify exciton-exciton interactions in QDs. However, the few available theoretical studies on this topic<sup>16–20</sup> have yielded conflicting results regarding both the sign (repulsion vs attraction) and the magnitude of the exciton-exciton interaction energy, highlighting the need for experimental benchmarks. Early experimental attempts to address this problem relied on indirect transient absorption measurements applied to QD/glass composites with relatively poor QD size monodispersity ( $>20\%$  size dispersion).<sup>21,22</sup> These experiments, along with more recent work on epitaxial CdSe QDs,<sup>23</sup> provided indications for a strong enhancement in the biexciton binding energy in QDs compared to bulk CdSe.

By applying our ultrafast PL experiments to a set of almost monodisperse QD samples spanning a wide range of sizes, we directly evaluate the magnitude and the size dependence of the exciton-exciton interaction energy. The shift of the biexciton emission band with respect to the single-exciton peak ( $\Delta_{XX}$ ) is determined by the sum of the exciton-exciton interaction energy ( $\delta E_2$ ) and the relaxation energy of the exciton that is created as a result of biexciton decay. If we assume that the biexcitons preferentially decay into ground state, relaxed excitons (as suggested, e.g., by calculations in Ref. 17), the “biexcitonic” shift  $\Delta_{XX}$  provides a direct measure of the biexciton binding energy.

The QD size-dependent biexcitonic shift (presumably equivalent to  $\delta E_2$ ) is plotted in Fig. 3(a). For the largest dots studied in this work ( $r = 35$  Å),  $\Delta_{XX} = 14$  meV, which is close to the bulk exciton binding energy and several times greater than the binding energy of a bulk biexciton. As the dot size is decreased, the binding energy first increases up to 33 meV at  $r = 18$  Å, then it starts to decrease and is approximately 12 meV for  $r = 11$  Å. The initial increase of  $\Delta_{XX}$  follows the  $1/r$  dependence (dashed line) as expected for exciton-exciton Coulomb interactions. The opposite trend observed at very small sizes likely results from repulsive electron-electron and hole-hole interactions that overwhelm the exciton-exciton attraction in the regime of extremely strong spatial confinement.<sup>18</sup>

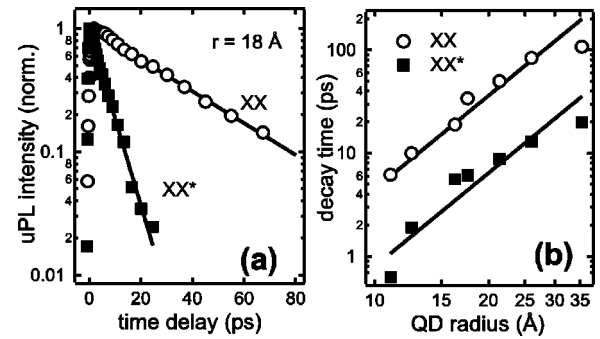


FIG. 4. (a) Neutral and charged biexciton dynamics for QDs with  $r = 18$  Å after subtracting a slowly decaying background due to single exciton decay. (b) Neutral (circles) and charged (squares) biexciton lifetimes as a function of QD radii fit to the  $r^3$  dependence.

To estimate the interaction energy of a charged biexciton state, we find the difference between energy of the  $XX^*$  band and the energy of the  $1P$  single exciton. Because of the extremely fast  $1P$ -to- $1S$  relaxation in the single exciton regime,<sup>11</sup> the latter quantity cannot be measured experimentally. Therefore, we estimate it as the sum of the measured  $1S$  exciton energy (the center of the uPL band at long times after excitation) and the energy spacing between the  $1S$  and  $1P$  electronic states from Ref. 24. For sizes from 35 to 18 Å, for which we were able to resolve the  $XX^*$  feature, the interaction energy  $\Delta_{XX^*}$  of the  $XX^*$  state steadily increases from 70 to 330 meV. Extremely large magnitudes of  $\Delta_{XX^*}$  likely result from large densities of uncompensated positive and negative charges within the  $XX^*$  species. These large charge densities are generated because of strongly different spatial distributions of electron (involving both  $1S$  and  $1P$  states) and hole (involving  $1S$  and surface states) wave functions.

The uPL experiment allows us also to directly measure lifetimes of multiexciton states (Fig. 4). Because of highly efficient Auger recombination, the decay of neutral and charged biexcitons is very fast and occurs on sub-100 ps time scales [Fig. 4(a)]. The decay time constant for both neutral and charged biexcitons exhibits the  $r^3$  dependence on the QD size [Fig. 4(b)], consistent with results of previous transient absorption studies.<sup>6</sup> As the dot size decreases from 35 to 11 Å the neutral biexciton life time shortens from 100 to 6 ps; and these time constants are close to those reported in Ref. 6 for two-pair states. The time constant for charged biexcitons varies from 20 to 0.7 ps for the same range of sizes. Interestingly, the Auger decay of charged biexcitons occurs much faster than the decay of neutral biexcitons. This difference likely results from stronger exciton-exciton interactions characteristic of charged species.

The large interaction energies measured in this work provide an interesting opportunity for achieving lasing in ultrasmall, sub-10 nm QDs in the single-exciton regime. In the absence of Coulomb interactions, the optical gain in these QDs develops at excitation densities  $\bar{N} > 1$ , implying that light amplification is provided by doubly excited nanoparticles (i.e., biexcitons). However, if exciton-exciton interactions are present in the system and the biexcitonic shift is

greater than the transition linewidth, the gain threshold can be achieved for  $\overline{N} > 2/3$ , i.e., before the onset of biexciton generation. If the above conditions are met (through, e.g., improved sample monodispersity and, possibly, engineered biexcitonic interactions), one could solve a major problem in the field of nanocrystal QD lasing, namely the ultrafast gain decay due to multiparticle Auger recombination.

In conclusion, by applying an ultrafast, PL up-conversion technique, we are able to detect the emission from short-lived neutral and charged biexcitons in ultrasmall CdSe nanocrystals with radii from 1.1 to 3.6 nm ( $0.2\text{--}0.8a_B$ ). The analysis of the spectral characteristics of the emission indicates that both types of biexcitons are characterized by extremely large interaction energies that are on the order of tens and hundreds of meV, for neutral and charged species, respectively. These values are much greater than the biexciton

binding energy in bulk CdSe (4.5 meV) indicating a significant increase in Coulomb exciton-exciton interactions induced by strong quantum confinement. The biexciton states show extremely fast relaxation dynamics. The observed decay constants scale proportionally to the nanocrystal volume and are in the range from 6 to 100 ps for neutral biexcitons and from 0.7 to 20 ps for charged biexcitons. These ultrafast relaxation dynamics are due to highly efficient Auger recombination resulting from strong interparticle Coulomb interactions.

This work was supported by Los Alamos Directed Research and Development Funds, and the Chemical Sciences, Biosciences and Geosciences Division of the Office of Basic Energy Sciences, Office of Science, U. S. Department of Energy.

- 
- <sup>1</sup>N. F. Mott, *Metal-insulator Transitions* (Taylor and Francis, London, 1974).
- <sup>2</sup>V. I. Klimov, A. A. Mikhailovsky, S. Xu, A. Malko, J. A. Hollingsworth, C. A. Leatherdale, H.-J. Eisler, and M. G. Bawendi, *Science* **290**, 314 (2000).
- <sup>3</sup>A. A. Mikhailovsky, A. V. Malko, J. A. Hollingsworth, M. G. Bawendi, and V. I. Klimov, *Appl. Phys. Lett.* **80**, 2380 (2002).
- <sup>4</sup>G. Chen, N. H. Bonadeo, D. G. Steel, D. Gammon, D. S. Katzer, D. Park, and L. J. Sham, *Science* **289**, 1906 (2000).
- <sup>5</sup>O. Benson, C. Santori, M. Pelton, and Y. Yamamoto, *Phys. Rev. Lett.* **84**, 2513 (2000).
- <sup>6</sup>V. I. Klimov, A. A. Mikhailovsky, D. W. McBranch, C. A. Leatherdale, and M. G. Bawendi, *Science* **287**, 1011 (2000).
- <sup>7</sup>J. Shah, *IEEE J. Quantum Electron.* **24**, 276 (1988).
- <sup>8</sup>V. I. Klimov, *J. Phys. Chem. B* **104**, 6112 (2000).
- <sup>9</sup>S. A. Crooker, T. Barrick, J. A. Hollingsworth, and V. I. Klimov, *Appl. Phys. Lett.* **82**, 2793 (2003).
- <sup>10</sup>The linewidths of the multiexciton bands are comparable to the width of the single-exciton emission spectrum, suggesting that there is no size selection within the quasi-monodisperse ensemble during the generation of multiexcitons. Therefore, the ensemble mean multiexciton emission energies can be characterized by the centers of the XX and XX\* bands.
- <sup>11</sup>V. I. Klimov and D. W. McBranch, *Phys. Rev. Lett.* **80**, 4028 (1998).
- <sup>12</sup>S. H. Park, R. A. Morgan, Y. Z. Hu, M. Lindberg, S. W. Koch, and N. Peyghambarian, *J. Opt. Soc. Am. B* **80**, 2097 (1990).
- <sup>13</sup>M. Nirmal, B. O. Dabbousi, M. G. Bawendi, J. J. Macklin, J. D. Trautman, T. D. Harris, and L. E. Brus, *Nature* **383**, 802 (1996).
- <sup>14</sup>T. D. Krauss, S. O'Brian, and L. E. Brus, *J. Phys. Chem. B* **105**, 1725 (2001).
- <sup>15</sup>H. Shionoya, H. Saito, E. Hanamura, and O. Akimoto, *Solid State Commun.* **12**, 223 (1973).
- <sup>16</sup>A. I. L. Efros and A. V. Rodina, *Solid State Commun.* **72**, 645 (1989).
- <sup>17</sup>J. Shumway, A. Franceschetti, and A. Zunger, *Phys. Rev. B* **63**, 155316 (2001).
- <sup>18</sup>T. Takagahara, *Phys. Rev. B* **39**, 10206 (1989).
- <sup>19</sup>L. Banyai, *Phys. Rev. B* **39**, 8022 (1989).
- <sup>20</sup>Y. Z. Hu, M. Lindberg, and S. W. Koch, *Phys. Rev. B* **42**, 1713 (1990).
- <sup>21</sup>K. I. Kang, A. D. Kepner, S. V. Gaponenko, S. W. Koch, Y. Z. Hu, and N. Peyghambarian, *Phys. Rev. B* **48**, 15449 (1993).
- <sup>22</sup>V. Klimov, S. Hunsche, and H. Kurz, *Phys. Rev. B* **50**, 8110 (1994).
- <sup>23</sup>V. D. Kulakovskii, G. Bacher, R. Weigand, T. Kummell, A. Forchel, E. Borovitskaya, K. Leonardi, and D. Hommel, *Phys. Rev. Lett.* **82**, 1780 (1999); G. Bacher, R. Weigand, J. Seufert, V. D. Kulakovskii, N. A. Gippius, A. Forchel, K. Leonardi, and D. Hommel, *ibid.* **83**, 4417 (1999).
- <sup>24</sup>P. Guyot-Sionnest and M. A. Hines, *Appl. Phys. Lett.* **72**, 686 (1998).